MATHEMATICAL MODELLING OF REMOTE DETECTION OF MOLECULAR AIR POLLUTANTS

František ZRCEK and Milan HORÁK

The J. Heyrovský Institute of Physical Chemistry and Electrochemistry, Czechoslovak Academy of Sciences, 118 40 Prague 1

Received April 1st, 1986

A model of remote detection of molecular air pollutants is devised based on the lidar equation. The various kinds of interaction of radiation with matter, *viz.* absorption, induced fluorescence, and Raman scattering, are taken into account; detection of either scattered or reflected signal is considered. The reflection is assumed to be either axial, using a retroreflector, or omnidirectional from a field target. Based on this model, an algorithm was set up for simulation of the different variants of the experiment, making allowance for a generally variable concentration of the compound along the optical pathway of the light beam. The basic atmospheric processes, *viz.* radiation absorption by the background, heat emission, turbulence, and the effect of atmospheric aerosols, are treated, and the last of them is found to play the major role. Aerosols are looked upon as a source of the Mie scattering and they are described by distribution equations with respect to the particle size and the complex refractive index. The variable concentration of the aerosol along the optical pathway and the simultaneous effect of a higher number of aerosol types are included.

Methods of remote sensing and monitoring have been developed to assist the study of the air composition and its local variations. They are based on the use of active sources of radiation, namely, intense laser beams which may or may not be tunable over a spectral region. This instrumentation is referred to as lidars (an acronym for *Li*ght *D*etection *a*nd *R*anging). The radiation emitted into the air interacts with the molecules and aerosols present, which leads to its scattering (Rayleigh or Raman scattering on molecules or Mie scattering on aerosols), absorption, or induced fluorescence. Detected is the signal over a suitably chosen wavelength range, either as scattered radiation along the optical pathway of the beam, or after reflection on a solid body, *e.g.*, a retroreflector. The signal transmits information about the target region, it can be, however, modified by the medium along the whole pathway.

The aim of the present work is to describe an algorithm set up for modelling all the variants of remote detection mentioned[1], allowing us to choose the optimum arrangement for the remote detection of some compounds in the air and, possibly, establishing their distribution along the optical pathway of the light beam. Only horizontal profiles are taken into account, *i.e.*, the temperature and pressure are regarded as constant and the composition of the majority air components as in-

variable. Details of the algorithm and the corresponding computer program are given in ref.[1]; in this work, stress is put on the various aspects of the model and phenomena affecting most the signal received, and examples of results of the modelling are given.

THEORETICAL

The Lidar Equation

The basic relation describing the propagation of a light beam through the atmosphere is the so-called lidar equation[2], relating the received energy (signal detected) E_d to the internal and external conditions of the experiment. The forms of this equation differ appreciably for the different variants of the experiment[1]; for instance, for the variant with reflected radiation the equation takes the simple form of

$$E_d = T_\lambda^2 T_p E_l(\tau_d/\tau_l)\, \xi\eta(\tau_d < \tau_l) \qquad (1)$$

(for the meaning of the symbols see the appended List of Symbols). Parameter η is the reflectivity of the retroreflector, *i.e.*, the fraction of radiation intensity observed after the axial reflection. If a target causing diffuse omnidirectional reflection is considered instead, this parameter is replaced by $A_p\varrho/(\pi W^2)$, the reflectivity of the target material ϱ being 0·3–0·05 according to the type of surface[3,4]; the lower values refer to the IR region.

During the detection of a scattered signal, the detector is hit simultaneously by radiation from an optical path segment $\Delta R = c\tau_l/2$, corresponding to one-half of the pulse length (assuming a rectangular pulse shape over the time τ_l). The signal is detected for a time τ_d, so that

$$E_\lambda = (E_l/\tau_l)\, A_p \overline{T}_p \int_t^{t+\tau_d} \xi(R')\, \mathrm{d}t' \int_{r_1(t')}^{r_2(t')} T_{\lambda_l} T_{\lambda_d} \sum_i \beta_i (\mathrm{d}r/r^2)\,, \qquad (2)$$

where $r_2 - r_1 = \Delta R$ and $R' = r(t') - c(\tau_l + \tau_d)/4$. If the transmission factors and backscatter coefficients β_i are considered variable, the integration is performed numerically, the overlap parameter $\xi(r)$, which is little dependent on r, being replaced by the $\xi(R')$ dependence.

The fluorescence induced by the beam exhibits its own time course, determined by the lifetime of the excited states τ_F which is negligible as compared to τ_l and τ_d. The number of excited molecules D^* can be regarded as negligible against the total number of molecules N of the interacting component. Then N is nearly equal to N_0, the number of molecules in the ground state, and the detector signal can be

described by a somewhat more complex general expression, similar, *e.g.*, to that given in ref.[5], *viz.*

$$E_d = E_l A_p[\sigma_F(\lambda_l)/(4\pi\tau_F)] \int_t^{t+\tau_d} \xi(R')\,dt' \int_{R_0}^{r_2(t')} N_0(r)\, T_{\lambda_l}(r)\, e^{-(\Delta t/\tau_F)} \cdot$$
$$\cdot \left(\int_{\lambda_{p_1}}^{\lambda_{p_2}} T_{\lambda_F}(r)\, T_p \zeta\, d\lambda' \right) (dr/r^2) \int_0^{\Delta t} j(x)\, e^{x/\tau_F}\, dx\,, \qquad (3)$$

where $\lambda_{p_2} - \lambda_{p_1} = \Delta\lambda_p$ and Δt is the time elapsed since the leading edge of the pulse passed the point with the coordinate r. The general form of the time course of the pulse j is normalized so that

$$\int_0^\infty j(x)\,dx = 1 \qquad (4)$$

(x is an auxiliary integration variable). R_0 is nearer to the rim of the cloud of the fluorescing component; actually, in view of the slow fluorescence extinction, the integration must be performed over the whole region from which the radiation hits the detector simultaneously (and which is generally larger than ΔR in Eq. (2)). The fact must also be considered that the fluorescence wavelength region $\Delta\lambda_F$ may be wider than the detected wavelength region $\Delta\lambda_p$, and the effectiveness in the region in question is given by the integral $\zeta(\lambda')$. The integrals in Eq. (3) must again be solved numerically.

Modelling the External Conditions of Experiment

The basic factor is the choice of the laser signal wavelength which mut lie within some of the so-called atmospheric windows, where no absorption of radiation by the majority components (carbon dioxide or water vapour) takes place[6]. The most important window is in the visible region, between 380 and 780 nm; on the short--wavelength side of this region, ozone and, farther, molecular oxygen and water vapour absorb, and at wavelengths shorter than 180 nm practically no measurement can be performed. In the IR region, carbon dioxide and, in particular, water vapour absorb appreciably, but a broad window exists in the 10 μm range. The atmosphere is virtually opaque to radiation wavelengths above 25 μm because of the immense absorption by water vapour. The large dipole moment of the water molecule gives rise to a high-intensity rotational spectrum encroaching on the centimetre wavelength region. In the boundary regions of the windows we considered "continuous" background absorption, given parametrically[7].

Rayleigh scattering on molecules of all air components plays a significant role in the visible spectral region. For the extinction coefficient α_R and the backscatter

coefficient β_R we have[8]

$$\alpha_R = (8\pi^3)/(3N_g\lambda_1^4)\,(n_g^2 - 1)^2\,(6 + 3\delta)/(6 - 7\delta) \tag{5}$$

and

$$\beta_R = (3/8\pi)\,\alpha_R\,, \tag{6}$$

where $\delta \approx 0{\cdot}035$. The atmospheric transmission factor component corresponding to Rayleigh scattering for the horizontal profile of the optical pathlength $2R$ is

$$T^R(\lambda_1, R) = \exp\left[2\alpha_R(\lambda_1)\,R\right]. \tag{7}$$

In the IR region this scattering can be disregarded, so that the scattered fraction is given by scattering on aerosols solely.

A next factor affecting the light beam during its passage through the air is the turbulence of the latter. This causes beam broadening (decolimation) and is a source of signal fluctuations. We proceeded from the weak fluctuations theory[9] when describing this effect. The increase in the beam radius $W(r)$ as compared to the radius in vacuum $W_0(r)$ is given by the relation

$$W^2(r) = W_0^2(r)/(1 - f)\,, \tag{8}$$

where

$$f = 2{\cdot}423C_n^2(2\pi/\lambda_1)^{1/3}\,r^{8/3}\left[W_0^2(r)\right]^{-5/6}. \tag{9}$$

The turbulence factor C_n^2 is within the limits of $10^{-17} - 10^{-12}$ $m^{-2/3}$. The transverse geometric beam profile was regarded as rectangular or Gaussian (symmetric about the beam axis).

The selective molecular absorption was assumed to obey the Lambert–Bouguer law in the form

$$T^A(\Delta\lambda_A, R) = \exp\left[-2\int_0^R \bar{\alpha}(\Delta\lambda_A)\,\mathrm{d}r\right] \tag{10}$$

for a finite width of the detectable wavelength range $\Delta\lambda_A$. At pressures in excess of about 5 kPa the Lorentzian shape allowing for the collision broadening[10] was considered. Eq. (*10*) can be exactly valid provided that spontaneous emission is negligible[11]. This is true if the optical thickness of the medium is lower than unity and the beam power density is lower than 10^7 W cm^{-1}.

The most intricate problem is in the modelling of the effect of aerosols. It turns out that it is just this effect that is decisive in most instances. Since the results of

calculation could not be confronted with experimental data, the conventional simple parametrization could not be applied. Therefore, we proceeded from the classical Mie scattering theory[12] which holds for single scattering on spherical particles. We employed the relative cross-sections of total extinction Q_{ext} and of backscattering Q_B, evaluated from summations of the Ricatti–Bessel functions for arguments $X = 2\pi a/\lambda$ and $Y = nX$, where $n = n - ik$ is the complex refractive index (the imaginary part represents the absorption). The extinction coefficients and backscatter coefficients of the individual, generally polydisperse, aerosols were evaluated as integrals over the distribution functions $N(a)$,

$$\alpha_M = \int_{a_1}^{a_2} N(a)\, Q_{ext}(X, Y)\, a^2\, da\,. \qquad (11)$$

The distribution functions used were dependences valid for Junge's, Deirmendjian's and the logarithmic-normal aerosol models[13,14]. The model can include as many as five types of independent aerosols, each of which can exhibit a variable concentration along the optical pathway, with a rectangular, linearly increasing, linearly decreasing, or Gaussian profile.

Mechanism of Detection of Molecular Compounds

The model comprises the methods of differential absorption, Raman scattering, and fluorescence. The method of differential absorption[15] is based on the alternate reception of two signals of mutually close wavelengths, one of which is in resonance with some of the absorption lines of the compound followed while the other is not. The method can be used either in combination with a reflective element at the end of the optical pathway or in the scattered signal detection arrangement. In the former case the average concentration of the compound in question along the optical pathway is obtained, in the latter case its spatial distribution can be derived in addition (using a pulse laser; a great deal of the signal intensity, however, is sacrificed).

Raman scattering[16] in the Stokes region can be also employed for concentration measurements, the signal detected, however, is very weak due to the very low differential cross-sections of Raman effect. Fluorescence measurements in a highly dense atmosphere suit to the monitoring of some selected compounds only, *e.g.* SO_2 or I_2, because of collision fluorescence quenching. Differential cross-sections for Rayleigh scattering, Raman scattering, and fluorescence are typically 10^{-26}, 10^{-29}, and 10^{-24} cm^2 sr^{-1}, respectively, differential cross-section for absorption is of the order of 10^{-20} cm^2.

It should be noted that the signal received by the detecting system contain an appreciable noise component arising from scattered solar radiation in the visible region and heat emission by the environment in the infrared region. The noise level

can attain values on the orders of magnitude of 10^{-5} W cm^{-2} sr^{-1} nm^{-1} in the 500 nm range and 10^{-3} W cm^{-2} sr^{-1} μm^{-1} in the 10 μm range.

RESULTS

Based on the concept dealt with in the preceding text, an algorithm for solving the different variants of the lidar equation and a Fortran program were set up and used to simulate atmospheric measurements. The parameters for the simulations were chosen so as to approach as closely as possible the actual conditions of remote air pollution monitoring, and particular attention was paid to the effect of atmospheric phenomena on the laser beam.

Effect of Atmospheric Phenomena

Atmospheric turbulence leads to nonlinear beam broadening in dependence on the C_n^2 value. For instance, at $\lambda = 10{\cdot}55$ μm the broadening was examined over the region of $C_n^2 \in \langle 10^{-11} - 10^{-16} \rangle$ m$^{-2/3}$ and found appreciable at $C_n^2 < 10^{-13}$ only; signal fluctuations then increase considerably. A correct description in terms of the weak fluctuations theory is possible at distances not exceeding approximately 2 000 m.

The effect of atmospheric aerosols is rather complex. The Q_{ext} values were compared to the published data available for various particle size and refractive index values[18], and no differences were observed. For X increasing beyond all bounds this value approaches two. Rapid oscillations of the values were found for Q_b at a low X and a real refractive index, which also agrees with published data. This effect is typical of spherical particles, where the angular part of the electromagnetic field forms standing waves on the particle surface. It was not established uniquely how this effect influences the data for poly disperse aerosols and to what extent the results of simulation will be affected.

Model Situations

Four simulations (denoted *I–IV*), "typical" of remote detection of molecules by lidar measurements in the air, are shown by way of illustration. System *I* simulates the method based on the Raman scattering measurement using an excimer laser; the subject of simulation is sulphur dioxide in a smoke plume (in a relatively high concentration of 0·5%) at a distance of hundreds of metres.

System *II* is used to document the expected sensitivity of the method of absorption of infrared radiation (about 10 μm wavelength) along the optical pathway to a distance of 3 km using a field reflector. Not very demanding instrumentation is required for the detection of a well-absorbing molecule (ethene) in concentrations below 1 ppm.

System *III* was designed to illustrate the method of differential absorption at two

close wavelengths, which is presumably the most popular approach. The treatment also documents the decisive effect of aerosols on measurements in the infrared spectral region.

System *IV* serves to assess the possibility of employing a fluorescence lidar for a selected compound, based on available data (sulphur dioxide in concentrations of units of ppm at distances up to 1 000 m).

The computer outputs for all the four cases are shown in Figs 1–4, respectively.

DISCUSSION

All results confirm the great effect of the presence and nature of aerosols in air, affecting the extinction and directly determining the backscattering in the infrared region. Only in the visible region, at wavelengths below 500 nm, Rayleigh scattering begins to play a role as well. For a theoretical prediction of a lidar experiment it would be thus desirable that the model of the aerosol should be better specified,

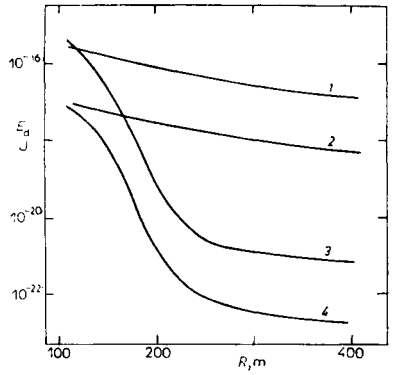

FIG. 1

System *I* — modelling Raman scattering by sulphur dioxide. Conditions: conc. SO_2 = = 0·5 vol. %, occurrence between 100 and 500 m, laser $E_l = 0{\cdot}25$ J, $\tau_l = \tau_d = 0{\cdot}32$ μs, $\lambda_l = 247$ nm, received wavelength $\lambda_d =$ = 254·6 nm, reference wavelength $\lambda_r =$ = 262·0 nm (Q-branch of N_2 band), cross-sections: SO_2 $6{\cdot}49 \cdot 10^{-29}$ cm^2 sr^{-1}, N_2 $1{\cdot}06 \cdot 10^{-29}$ cm^2 sr^{-1}. Curves: *1* N_2 (without aerosol), *2* SO_2 (without aerosol), *3* N_2 (with aerosol, extinction coefficient $\alpha = 5{\cdot}38 \cdot 10^{-4}$ cm^{-1} at 262 nm), *4* SO_2 (with aerosol, $\alpha = 5{\cdot}24 \cdot 10^{-4}$ cm^{-1} at 254·2 nm)

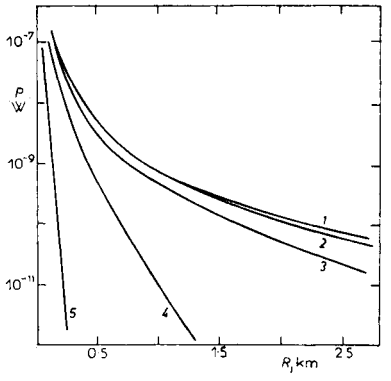

FIG. 2

System *II* — modelling absorption by ethene (use of a reflecting element). Conditions: reflectivity 5%, a continuous CO_2 laser 1 W power on a line at $\lambda = 10{\cdot}526$ μm, total background extinction $\alpha = 1{\cdot}245 \cdot 10^{-6}$ cm^{-1}, absorption cross-section $0{\cdot}17 \cdot 10^{-17}$ cm^2, conc. C_2H_4 (ppm): *1* 0, *2* 0·005, *3* 0·05, *4* 0·5, *5* 5

particularly by including aspherical particles as well, or that a particular situation with known extinction and backscatter coefficients should be treated.

Now, the individual detection arrangemets can be commented on as follows. Clearly the most sensitive is the measurement of differential absorption in a system with a reflecting element. Its sensitivity can be additionally increased to concentrations at the level of units of ppb by using a retroreflector. Differential absorption with the detection of the scattered signal is affected substantially by the presence of aerosols, particularly in the infrared region. If, however, a suitable wavelength pair is found for a tunable high-power laser, compounds at concentration levels of tens of ppm can be monitored in favourable circumstances. In some cases, the fact that the measured signal is lower than the reference signal is a drawback of this method.

The Raman scattering and fluorescence methods are clearly of lesser importance for remote detection in dense atmospheres. The former is low sensitive, even if the excimer laser, as treated by us, is replaced by a nitrogen laser which at higher wave-

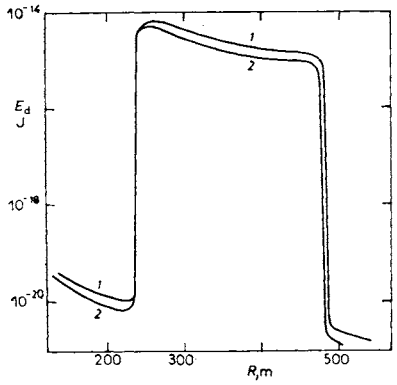

FIG. 3

System *III* — modelling differential absorption during measurement of scattered radiation. Conditions: a CO_2 laser, $E_l = 1$ J, $\tau_l = \tau_d = 0{\cdot}1$ μs, measured wavelength $\lambda = 10{\cdot}528$ μm, reference wavelength $\lambda_r = 10{\cdot}62$ μm, aerosol I $\alpha = 3{\cdot}07 . 10^{-14}$ cm^{-1}, $\beta = 8{\cdot}38 . 10^{-15}$ cm^{-1} sr^{-1}, constant profile; aerosol II $\alpha = 4{\cdot}67 . 10^{-6}$ cm^{-1}, $\beta = 5{\cdot}75 . 10^{-8}$ cm^{-1} sr^{-1}, rectangular profile, occurrence between 220 and 450 m. Curves: *1* signal without absorption, *2* absorption by 5 ppm ethene (constant profile)

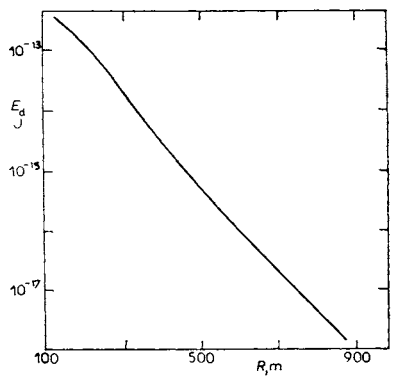

FIG. 4

System *IV* — modelling induced fluorescence of sulphur dioxide. Conditions: laser $E_l = 1$ J, $\tau_l = 0{\cdot}1$ μs, $\tau_d = 0{\cdot}2$ μs, emitted wavelength $\lambda_l = 300{\cdot}1$ nm, received wavelength $\lambda_d = 310$ nm (30% radiation within the range of $\Delta\lambda = 10$ nm); excited state lifetime $\tau_F = 0{\cdot}21 . 10^{-8}$ s, total background extinction $\alpha = 1{\cdot}061 . 10^{-5}$ cm^{-1}. Curve: 5 ppm SO_2, rectangular profile from 100 m on

lengths offers a higher power in shorter pulses. The sensitivity of the method is at a concentration level of units per cent. A remarkable asset of this method is in the fact that the constant concentration of nitrogen in air can serve as an internal standard for quantitative measurements.

The modelling of the fluorescence experiment was performed by way of illustration, no unique conclusions, however, can be drawn because of the lack of requisite data such as the collision factors under atmospheric conditions.

LIST OF SYMBOLS

A_p area of receiver optics, m^2
a aerosol particle size parameter, m
C_n^2 atmosphere turbulence factor, $m^{-2/3}$
c light velocity, $m\ s^{-1}$
E_d energy hitting the detector, J
E_l pulse energy, J
j pulse time characteristics, s^{-1}
k imaginary part of refractive index
N total number of molecules of component, m^{-3}
$N(a)$ distribution function of aerosol with respect to parameter a, m^{-4}
N_g number of molecules in atmosphere
N_0 number of molecules in ground state
N^* number of excited molecules
n real part of refractive index
n_g refractive index of atmosphere
n complex refractive index
Q_{ext} relative cross-section of spherical aerosol for total extinction
Q_B relative cross-section of spherical aerosol for backscattering
R optical pathway, m
ΔR optical pathway segment from which signal is received simultaneously, m
r variable along the optical pathway, m
T_p transmission factor of receiver optics
T_λ transmission factor of atmosphere at wavelength λ
t time, s
W beam radius broadened by turbulence, m
W_0 beam radius in vacuum, m
X, Y relative cross-section parameters
α extinction coefficient, m^{-1}
β backscatter coefficient, $m^{-1}\ sr^{-1}$
η retroreflector reflectivity (axial reflection)
δ depolarization factor of atmosphere
λ wavelength, m
λ_l wavelength of radiation emitted by laser, m
λ_p wavelength of radiation detected after interaction with atmosphere, m
$\Delta\lambda$ wavelength range, m
λ' variable in wavelength range, m
ξ parameter of overlap of irradiated region and region wherefrom signal is received

ϱ backreflectivity of target material
σ_F fluorescence cross-section, m^2
τ_d time constant of detector, s
τ_l pulse length, s
τ_F lifetime of excited state of molecule, s
φ distribution function of radiation intensities over the wavelength region (ν, ∞), m^{-1}

REFERENCES

1. Zrcek F.: *Thesis.* Prague 1984.
2. Measures R. M. in the book: *Analytical Laser Spectroscopy* (N. Omenetto, Ed.), p. 295 to 411. Wiley, New York 1979.
3. Wolfe W. L.: *Handbook of Military IR Technology.* U.S. Government Printing Office 1978.
4. Kaminski W. R.: *CO_2 Laser Devices and Applications.* SPIE 227, 1980.
5. Measures R. M.: Appl. Opt. *16*, 1092 (1977).
6. Hanst P. L.: Appl. Spectrosc. *24*, 161 (1970).
7. Tuer T. W. and coworkers: *Atmospheric Effects on Low-Power Laser Beam Propagation.* NRCAA MI U.S.A. Report 1980.
8. Zuev V. E. in the book: *Laser Monitoring of the Atmosphere* (E. D. Hinkley, Ed.). Springer, Berlin 1976.
9. Ishimaru A. in the book: *Laser Beam Propagation in the Atmosphere* (J. W. Strohbehn, Ed.), p. 169. Springer, Berlin 1978.
10. Horák M., Vítek A.: *Interpretation and Handling of Vibrational Spectra.* Wiley, Chichester 1978.
11. Papoušek D., Urban Š.: Chem. Listy *76*, 404 (1982).
12. Kerker M.: *The Scattering of Light and Other Electromagnetic Radiation.* Academic Press, New York 1969.
13. McCartney E. J.: *Optics of the Atmosphere. Scattering by Molecules and Particles.* Wiley, New York 1977.
14. Deirmendijan D.: *Electromagnetic Wave Scattering on Spherical Polydispersions.* American Elsevier, New York 1969.
15. Schotland R. M.: *Proc. 4th Symp. on Remote Sensing. University of Michigan 1966.*
16. Melfi S. H., Brumfield M. L., Storey K. W.: Appl. Phys. Lett. *22*, 38 (1973).
17. Inaba H. in the book: *Laser Monitoring of the Atmosphere* (E. D. Hinkley, Ed.), p. 153. Springer, Berlin 1976.
18. Van de Hulst H. C.: *Light Scattering by Small Particles.* Wiley, New York 1957.

Translated by P. Adámek.